

THE ROTATION CURVES OF GALAXIES AT INTERMEDIATE REDSHIFT¹

Nicole P. Vogt and Terry Herter

Center for Radiophysics and Space Research, Cornell University, Ithaca, NY 14853

Martha P. Haynes

Center for Radiophysics and Space Research, Cornell University and National Astronomy
and Ionosphere Center², Ithaca, NY 14853

and

Stéphane Courteau

Center for Radiophysics and Space Research, Cornell University, Ithaca, NY 14853

Received 7 June 1993; accepted 16 July 1993

Accepted for publication in *The Astrophysical Journal Letters*

¹Based on observations made at the Palomar Observatory as part of a continuing collaborative agreement between the California Institute of Technology and Cornell University.

²The National Astronomy and Ionosphere Center is operated by Cornell University under a management agreement with the National Science Foundation.

ABSTRACT

We have undertaken a pilot project to measure the rotation velocities of spiral galaxies in the redshift range $0.18 \leq z \leq 0.4$ using high dispersion long slit spectroscopy obtained with the Palomar 5m telescope. One field galaxy and three cluster objects known to have strong emission lines were observed over wavelength ranges covering the redshifted lines of [OII], CaII K, $H\beta$, and [OIII]. Two of the objects show extended line emission that allows the tracing of the rotation curve in one or more lines. A line width similar to that obtained with single dish telescopes for the 21-cm HI line observed in lower redshift galaxies can be derived from the observed $H\beta$, [OII], and [OIII] emission by measuring a characteristic width from the velocity histogram. These moderately distant galaxies have much stronger emission lines than typical low-redshift spirals but they appear to be kinematically similar. Application of the Tully-Fisher relation suggests that the two galaxies with rotation curves are intrinsically brighter at R-band than nearby galaxies.

Subject headings: galaxies: distances and redshifts – galaxies: evolution – galaxies: kinematics and dynamics

1. Introduction

A major goal of cosmology is to determine the temporal history and fate of the universe. Galaxies provide the primary means to accomplish this; thus it is critically important to understand their formation and evolution. Between the present time and the epoch corresponding to a redshift $z \simeq 0.4$, significant evolution of the cluster population results in a higher fraction of blue galaxies at the earlier epoch. Most recent high resolution imaging of the blue cluster members confirms their spiral nature (Lavery *et al.* 1992; Dressler *et al.* 1993). A number of authors conclude that galaxy–galaxy interactions play a primary role in producing an enhancement in the blue galaxy fraction in distant clusters (Thompson 1988; Lavery and Henry 1988; Lavery *et al.* 1992) while others suggest that the excess activity in blue galaxies is associated with the interaction between hot intracluster gas and infalling galaxies (Dressler *et al.* 1985; Bothun and Dressler 1986). The detailed study of the kinematics of the blue cluster galaxies and their counterparts in the field at similar redshifts will place constraints on both the formation and evolutionary processes.

In recent years, the HI Tully–Fisher (TF) relation and its optical analog have been used by a growing community in attempts to map out the local flow field. These peculiar motions hinder determination of the Hubble constant from nearby galaxies. However, at distances larger than $z \simeq 0.04$, peculiar motions should be negligible with respect to the overall Hubble flow and the main source of error is the intrinsic scatter in the TF relation (about 0.3 mag) and the local calibration. Thus, if the TF method can be properly understood and applied, it may permit the determination of redshift–independent distances and evaluation of the Hubble constant, at intermediate redshift.

The prospects for high redshift application of the TF method using the $H\alpha$ line

have been discussed by van der Kruit and Pickles (1988). Detection of the $H\alpha$ line as the distance to the emitting object increases is hampered not only by the radial fall-off in emissivity but also because the redshifting of the line from its rest wavelength places the $H\alpha$ line in the night-sky-contaminated red portion of the spectrum until it finally moves out of the optical window at $z \geq 0.4$. An alternative approach, discussed in the context of star formation indicators by Kennicutt (1992a,b), relies on lines whose rest wavelengths are significantly lower than that of $H\alpha$, specifically, the emission lines of [OII], $H\beta$, and [OIII]. All three lines are often (though *not always*) seen in the spectra of nearby spiral galaxies, the same objects in which $H\alpha$ is detected.

In this *Letter*, we report the results of a pilot project to conduct high resolution, high-sensitivity long-slit spectroscopic observations of galaxies in the redshift range $0.18 \leq z \leq 0.4$. In § 2 we discuss our observational strategy. A summary of the results, including the extended rotation curves of two galaxies with $z \simeq 0.2$, is presented in § 3. Finally, we discuss the degree of success of our experiment and the potential for using this technique to derive an estimate of the Hubble constant out to such distances.

2. Observations

Since our objective was to ensure the greatest likelihood for measuring rotation curves we chose objects in the redshift range 0.2 – 0.4 known to have strong emission lines and displaying an optical appearance suggestive of spiral morphology. Final observations were constrained by the specific time available for observation which was primarily determined by weather conditions.

Long-slit spectra were taken with the Hale 5m telescope using the Double Spectrograph (Oke and Gunn 1982) in November 1992 and January 1993. Simultaneous

blue (3100 – 5200 Å) and red (5200 – 11000 Å) spectra were obtained with 1200 l/mm gratings and the Palomar D52 dichroic beam splitter. A 1" slit was used for the observations. The blue and red camera have a spatial scale of 0.78"/pixel and 0.58"/pixel, and a dispersion of 0.56 Å/pixel and 0.82 Å/pixel respectively. We observed the resolved [OII] doublet ($\lambda 3726$, $\lambda 3729$) in the blue camera, and the [OIII] line pair ($\lambda 4959$, $\lambda 5007$), and $H\beta$ ($\lambda 4861$) with the red camera.

An accurate determination of source coordinates proved to be essential to the success of this project. Coordinates for surrounding stars were taken from the HST Guide Star Catalog and applied exactly to create a transformation matrix for images of the clusters into right ascension and declination. We obtained very accurate relative coordinates between our target sources, the other galaxies in the cluster, and the neighboring guide stars.

The ~ 21 st magnitude sources were completely invisible to the guider camera when in the slit, and by mischance no stars fell within the fields of view on our exposures. During both observing runs weather conditions were somewhat variable, and the seeing conditions ranged from sub-arcsecond to greater than 1.5". Under poor seeing conditions ($> 1''$) we repeatedly halted the exposures and returned to the guide star to correct for possible drift, every ten to twenty-five minutes depending upon the wind conditions and the hour angle of the telescope. When the seeing was sub-arcsecond and it was completely clear, we were able to guide readily on companion galaxies within the cluster. To achieve adequate signal-to-noise in the extended emission (based on experiences observing lower redshift galaxies) exposure times of two hours were used, weather permitting. These times and a rough estimate of the seeing quality for the four distant galaxies for which we obtained adequate data are included with other relevant information in Table 1.

3. Results

We performed the data reduction within the IRAF programming environment, using standard packages for the initial stages and then linked FORTRAN programs to fit a Gaussian profile to the line at each spatial position. The [OII] doublet and [OIII] line pair were each fit as a double Gaussian profile. The error bars on the rotation curves displayed in figures 1 and 3 reflect the quality of the Gaussian fits to the data; we believe them to be larger than any systematic errors. The velocity scales on the y-axis measure the rotational velocity of the galaxy about an estimated central point *in the rest frame of the galaxy*. A characteristic velocity width, W , is derived from a histogram of the velocity distribution and is the full width measured across the inner 80% of the histogram area. No intensity weighting is performed. This width is consistent with those estimated from fitting the maximum of the rotation curve and from visual inspection of the rotation curves. Since each of the current observations is distinct in terms of both intrinsic nature and degree of success, we discuss the results separately.

Galaxy 2545.3 in SA 68: The first object is a strong emission line galaxy from the SA 68 field sample of Koo (1985). The particular object designated 2545.3 ($z = 0.211$) was chosen because it has very strong emission of [OII], $H\beta$, and [OIII]. The morphology of the object is difficult to establish on a photographic plate made available by Koo and Ellman but it appears elongated with a small bulge. It is clearly unusual given the strength of its emission lines.

Figure 1 shows the observed variation in velocity as derived for the [OII] and [OIII] separately. As a demonstration of the data quality, Figure 2 presents the spectral image of the resolved [OII] doublet. An unexpected companion source was detected $2''$ away

on the sky, an order of magnitude weaker with no distinguishing features. The full optical extent of the galaxy can be seen in [OII], $H\beta$, and [OIII], though the red-shifted $H\beta$ line falls directly upon a broad OH night sky line from which it proved to be inseparable. All four oxygen lines are quite strong. As seen in Figure 1, the rotation curve is quite symmetric, and both lines give consistent results. The velocity widths determined independently from each set of lines agree to within 10 km s^{-1} , giving a final value of $115 \pm 5 \text{ km s}^{-1}$ for W. The inclination of the galaxy, determined from digitized 4m photographic plate material is $44^\circ \pm 3^\circ$, yielding a corrected width W_c of $166 \pm 13 \text{ km s}^{-1}$.

Galaxies No. 57 and No. 208 in CL 0949+44: We detected two galaxies in the cluster CL0949+44 at $z = 0.380$, selected for the presence of strong emission from the spectroscopic catalog of Dressler and Gunn (1992). As discussed by Dressler and Gunn, this cluster actually contains two separate velocity components and is populated by the bluest galaxies in their cluster sample.

Galaxy No. 57 was detected in [OII], [OIII], and $H\beta$. Though the signal-to-noise ratio is quite good we can see little extension beyond the nuclear region of the galaxy. The width of the emission lines in the nucleus, on the order of 150 km s^{-1} , suggest that this is a Seyfert class object (Osterbrock 1989). Dressler and Gunn (1992) classify this object as having an exponential light distribution. It appears roughly spherical in Figure 1 of Dressler and Gunn (1992) and lies at some distance from the cluster core.

Galaxy No. 208 is the object used by Dressler and Gunn in their Figure 8 as an example of an emission-line galaxy. We detected both oxygen lines and $H\beta$, but no emission was detectable beyond the nucleus. It appears roughly spherical and the light profile follows a $r^{1/4}$ law.

BOW No. 85 in Abell 963: Our final source is a member of the rich cluster Abell

963 at $z = 0.201$, labeled No. 85 in the catalog of Abell 963 presented by Butcher *et al.* (1983; hereafter BOW). We successfully traced the extent of the [OII] doublet, and detected the fainter $H\beta$ and [OIII] lines. The variation in velocity along the major axis drawn from the [OII] data is presented in Figure 3. We derive a velocity width W of $230 \pm 8 \text{ km s}^{-1}$.

Lavery and Henry (1988) obtained spectra and images of this blue emission–line galaxy. Their spectrum shows strong [OII] and [OIII] emission lines as well as high order Balmer absorption lines. Their image clearly indicates that the object is elongated, suggesting its spiral nature. Although their image is not very deep, they suspect tidal interaction between this galaxy and a companion about $4''$ to the north. Using their image to estimate an axial ratio of 0.44, we derive a corrected velocity width W_c of $253 \pm 8 \text{ km s}^{-1}$.

4. Discussion

The results of this pilot effort demonstrate the potential of investigating the kinematics of galaxies at intermediate redshift via long–slit spectroscopy. Given very good seeing ($< 1''$) and adequate weather conditions, this project confirms the efficacy of the measurement of rotation curves in distant galaxies. The rotation curves shown in figures 1 and 3 are well-defined and appear to flatten, characteristics seen in nearby normal spiral galaxies. At the same time the presence of strong emission in the objects makes them quite unusual compared to low redshift galaxies. Although both galaxies showing extended emission appear to have nearby companions, there is no evidence of interaction in their rotation curves.

In order to compare the extent of the rotation curve derived from the various lines,

we obtained similar high resolution long slit spectra for a small sample of relatively nearby, normal galaxies ($z \sim 0.02$) over wavelength ranges covering all of the relevant lines including $H\alpha$. Although the current sample is still small, primarily because of weather limitations, we note that the extent of the rotation curve traced in all lines is similar within the constraint that the signal-to-noise ratio is much higher for the $H\alpha$ emission. The velocity widths measured from different lines are consistent within the errors. In the nearby objects, the oxygen lines are far weaker than the $H\alpha$ line, but unlike our high z candidates these galaxies had not been pre-selected for strong oxygen emission.

Measurements of the velocity widths allow estimation of galaxy properties and/or distances via application of the TF relation. Since most TF studies of nearby galaxies have been calibrated using radio 21-cm line widths, the optical widths must be transformed to a system appropriate to the radio TF relation. This is particularly critical for distant studies where the velocity width rather than a detailed rotation curve may be all that is available. A relative calibration between optical and HI line widths has been derived from a sample of low redshift galaxies, most of them in nearby Abell clusters. Using 145 objects with both high quality HI line widths and optical velocity widths derived in the same manner employed here, we have derived a transformation relation between the optical width W and the 21-cm line width as used by Pierce and Tully (1988). Using this transformation, we derive an equivalent corrected (for turbulent broadening) 21-cm line width W_c^{21} of $185 \pm 15 \text{ km s}^{-1}$ for Galaxy 2545.3 and $264 \pm 11 \text{ km s}^{-1}$ for BOW 85. A more complete discussion of the comparison of radio and optical width measurements will be presented elsewhere (Vogt *et al.* 1993). The corrected 21-cm width derived for 2545.3 is rather small, particularly relative to the mean expected for a large sample of low redshift objects (Roberts and Haynes 1993). It is possible, given the uncertainties, that this object may be less inclined than the

current estimate, or that the rotation curve continues to rise significantly, beyond the radius at which line emission is detected.

Using the TF relation, the intrinsic brightness of distant galaxies can be compared, albeit crudely, to those nearby. Using the R-band calibration of the TF relation by Pierce and Tully (1988), a Hubble constant of $75 \text{ km s}^{-1} \text{ Mpc}^{-1}$, and the Scd galaxy energy distribution of Pence (1976) for the K-correction, we estimate that BOW 85 and 2545.3 are 0.9 ± 0.4 and 3.1 ± 0.7 magnitudes brighter respectively than predicted from the nearby galaxy sample. (Another 0.3 magnitude error should be added in quadrature with the quoted errors to account for the intrinsic scatter in the TF relation). Given the various uncertainties and complications in comparing the distant galaxies to the nearby ones, this increase in the brightness of distant galaxies relative to nearby ones of the same velocity width should be considered preliminary. Similar results have been reported by Franx (1993) who applied the luminosity–velocity dispersion relation to E+A galaxies in the cluster A665 at $z=0.18$.

Because of our galaxy selection process and the potential for galaxy evolution, use of the TF relation to derive a Hubble constant is not justified at this time. In the future a better statistical sample will allow a comparison of the slope of the TF relation at high and low redshift and the evaluation of the importance of merging in the blue galaxy population. High resolution images such as those obtained recently with HST by Dressler *et al.* (1993) will give better estimates of the galaxy morphologies and inclination angles. Multiband application of the TF relation will help to investigate galaxy evolution since long wavelengths should be progressively less affected by it. Alternatively, if the effects of galaxy evolution can be disentangled and the local calibration of the TF relation verified, the Hubble constant can be determined.

This work has been funded by NSF grants AST9014858 and AST9023450. S.C.

is also supported by a Canadian NSERC Postdoctoral Fellowship. We thank Nancy Ellman and David Koo for providing information concerning galaxy 2545.3 in SA68 and Marco Scodeggio for assistance in obtaining guide star candidates.

Table 1: Information on observed galaxies.

Field	Galaxy	RA			Dec			z	R^a	W^b	t^c	seeing	r^d	ref
		h	m	s	°	'	"							
SA68	2545.3	00	14	36.6	+17	00	32	0.211	3.5	115	2.0	1.5	18.4 ^e	1
CL0949	DG 57	09	49	42.7	+44	10	46	0.357	–	–	1.5	0.9	21.7	2
CL0949	DG 208	09	49	45.0	+44	08	14	0.380	–	150	2.0	1.1	21.3	2
A963	BO 85	10	14	11.7	+39	16	30	0.201	4.0	230	2.0	0.8	19.0 ^f	3

^aMaximum radial extent of detected emission.

^bOptical velocity width. See text for definition.

^cIntegration time.

^dGunn r band magnitude or its equivalent.

^eDerived from J magnitude of 20.12 from Ellman and Koo and assuming $\langle J-F \rangle = 1.4$ and $\langle V-R \rangle = 0.5$

^fDerived from F magnitude given by BOW using their conversion from F to R-band and assuming $\langle V-R \rangle = 0.5$.

References. — (1) Koo (1985), (2) Dressler and Gunn (1992), (3) Butcher, Oemler and Wells (1983).

REFERENCES

- Bothun, G and Dressler, A. 1986, *ApJ*, 301, 57.
- Butcher, H., Oemler, Jr. A., and Wells, D.C. 1983, *ApJS*, 52, 183.
- Dressler, A. and Gunn, J.E. 1992, *ApJS*, 78, 1.
- Dressler, A., Gunn, J.E. and Schneider, D.P. 1985, *ApJ*, 294, 70.
- Dressler, A., Oemler, A. Jr., Gunn, J.E. and Butcher, H. 1993, *ApJ*, 404, L45.
- Franx, M. 1993, *ApJ*, 407, L5.
- Kennicutt, R.C. 1992a, *ApJ*, 388, 310.
- Kennicutt, R.C. 1992b, *ApJS*, 79, 255.
- Koo, D.C. 1985, *AJ*, 90, 418.
- Lavery, R.J. and Henry, J.P 1988, *ApJ*, 330, 596.
- Lavery, R.J. Pierce, M.J. and McClure, R.D. 1992, *AJ*, 104, 2067.
- Oke, J.B. and Gunn, J.E. 1982, *PASP*, 94, 586.
- Osterbrock, D.E. 1989, *Astrophysics of Gaseous Nebulae and Active Galactic Nuclei* (Mill Valley: University Science Books), 312.
- Pence, W. 1976, *ApJ*, 203, 39.
- Pierce, M.J. and Tully, R.B. 1988, *ApJ*, 330, 579.
- Roberts, M.S. and Haynes, M.P. 1993, in preparation.
- Thompson, L.A. 1988, *ApJ*, 324, 112.

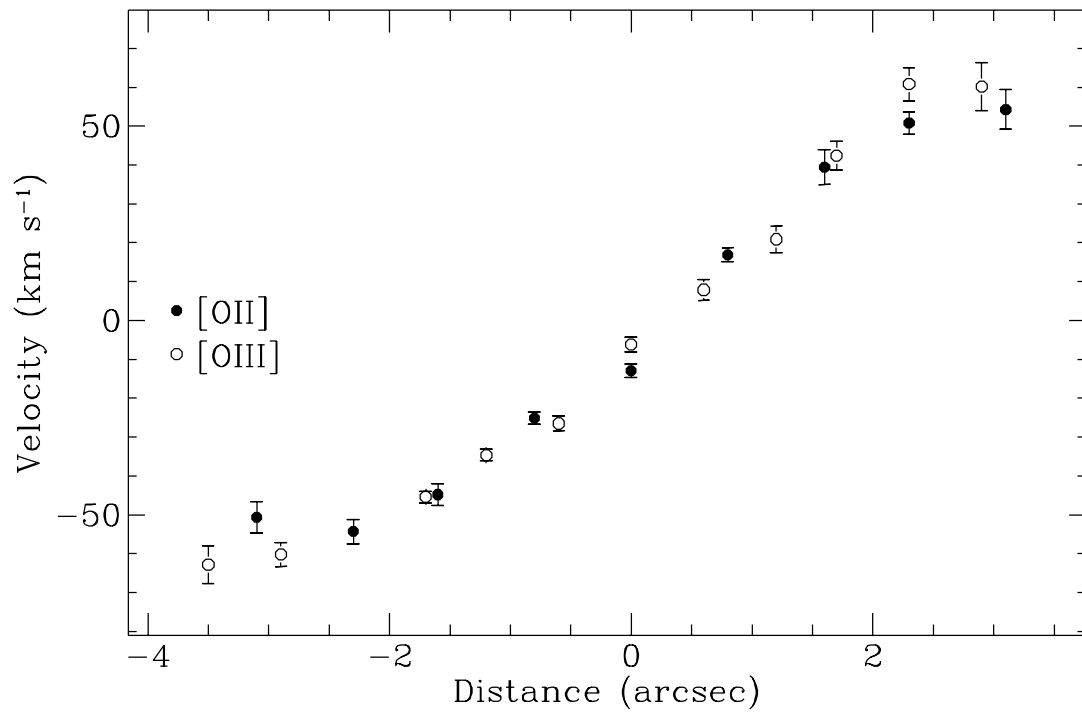
van der Kruit, P.C. and Pickles, A.J. 1988, in *Towards Understanding Galaxies at High Redshift*, ed. by R.G. Kron and A. Renzini (Kluwer; Hingham), p. 339.

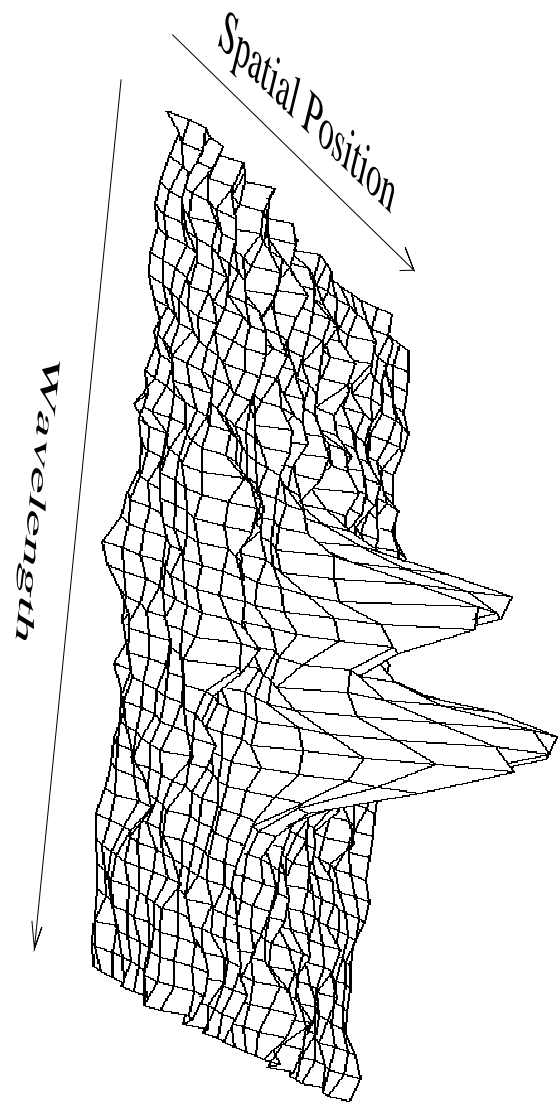
Vogt, N.P., Herter, T., Haynes, M.P. and Giovanelli, R. 1993, in preparation.

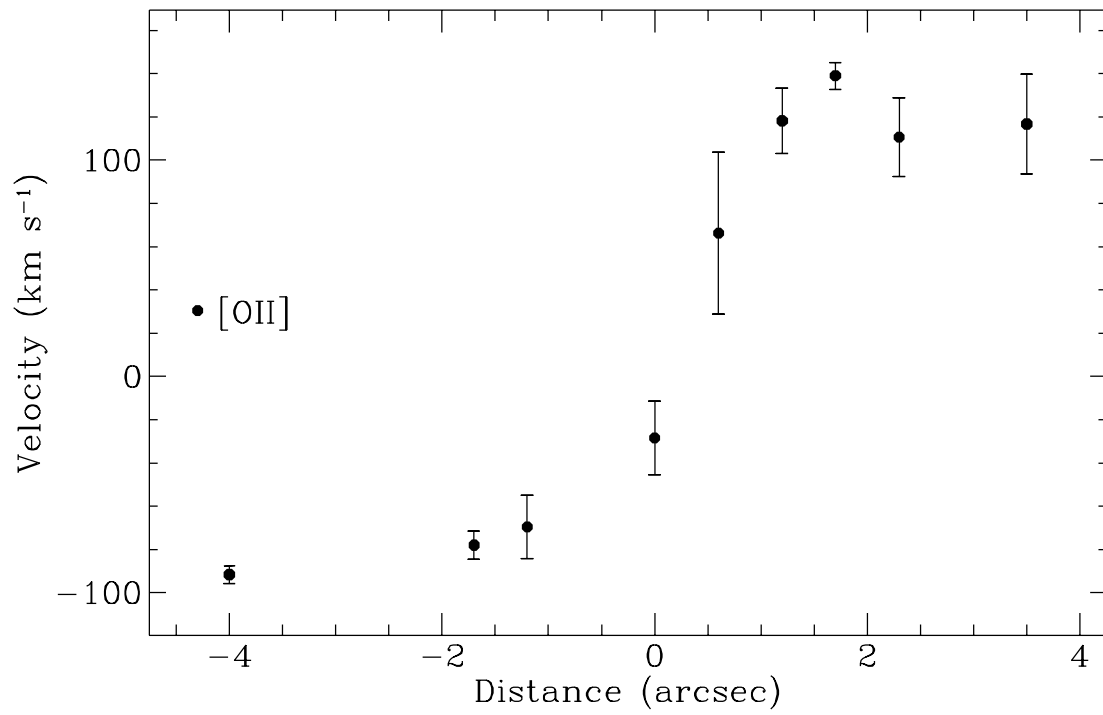
Fig. 1.— The spatial variation in the velocities in the rest frame of the galaxy derived from the [OII] and [OIII] line profiles for 2545.3 in the SA 68 field.

Fig. 2.— Spectral image of the resolved [OII] doublet ($\lambda 3726$, $\lambda 3729$) for the galaxy 2545.3 in the SA 68 field. The grid step is 0.56 \AA per pixel in the dispersion direction and $0.78''$ per pixel in the cross-dispersion direction. The peak intensity is $45\text{-}\sigma$ above the noise.

Fig. 3.— The spatial variation in the velocities in the rest frame of the galaxy derived from the [OII] line profiles for the No. 85 in Abell 963. The data at $-3''$ fell onto a bad column on the chip and was distorted.







-